

Cite this: *J. Mater. Chem. C*, 2019,
7, 13759Received 23rd September 2019,
Accepted 22nd October 2019

DOI: 10.1039/c9tc05218f

rsc.li/materials-c

Phenanthroimidazole derivatives with minor structural differences: crystalline polymorphisms, different molecular packing, and totally different mechanoluminescence†

Yun Yu,^a Yuanyuan Fan,^a Can Wang,^a Yao Wei,^a Qiuyan Liao,^a Qianqian Li^{id}^a and Zhen Li^{id}^{*ab}

Two crystalline polymorphs of tPTI-Bpin displayed opposite mechanoluminescence (ML) performance, and had different space groups of $P2_1/c$ (ML-active tPTI-B1) and $P\bar{1}$ (ML-inactive tPTI-B2), respectively. For comparison, another analogue molecule of PTI-Bpin was designed. Careful analysis of their crystal structures demonstrated that the special triangle-like molecular packing mode of tPTI-B1 mainly accounted for its distinctive ML behavior. Regardless of its minor difference in chemical structure from that of tPTI-Bpin, PTI-B without the ML property has similar parallelogram-like molecular packing to tPTI-B2, further confirming that the ML property is highly related to the molecular packing rather than the chemical structure.

Organic luminogens have attracted increasing interest due to their wide applications in OLEDs (organic light-emitting diodes), organic lasers, stimuli-responses, bioimaging and so on.¹ Besides the electronic nature of molecular structures, the molecular packing plays a key role in realizing high functional performance, exhibiting the Molecular Uniting Set Identified Characteristic (MUSIC).² As typical examples, the crystalline polymorphisms of organic molecules demonstrated different and even opposite properties, regardless of their same chemical structures.³ This case also occurred for purely organic luminogens with mechanoluminescence (ML), which is a unique light emission induced by external mechanical stimulation, but not normal photo excitation (Chart S1, ESI†).^{4,6} Thus, to realize good ML performance, the molecular packing of luminogens should be paid much attention, in addition to their chemical structures.

Thanks to the efforts of scientists, many luminogens with strong ML emissions have been reported, and the inherent mechanism has been explored step by step.⁵ And actually, the results from the crystalline polymorphism contribute much to the deep understanding of the interesting ML phenomena.⁶ Also, some isomers gave important information on the influence of the molecular packing on the ML property, in which the only difference is the linkage position of the aromatic blocks. For example, two isomers of a phenanthro[9,10-*d*]imidazole derivative exhibited opposite ML properties.⁷ Thus, all the cases of polymorphisms and isomers confirmed the importance of the molecular packing in addition to the molecular structure, demonstrating the urgent requirement for exploring the structure-packing-property relationship. Accordingly, more ML luminogens should be obtained to provide more information, especially those polymorphisms.

Analyzing the reported ML polymorphisms carefully, in many cases, the information of molecular packing was collected from just the two polymorphs of one ML luminogen, and there were no other analogues with minor structural differences for comparison, although some important information could be expected from the analogues. From this point, we would like to design polymorphs with ML properties and comparable analogues. Accordingly, based on our previous work, 1,2-diphenylphenamimidazole was selected as the basic aromatic ring, and the boronic ester group was introduced to construct tPTI-Bpin, since the aryl boronic ester group could benefit the ML property for its enhancement of the efficient intermolecular interactions.⁸ For comparison, PTI-Bpin was also synthesized, which had almost the same chemical structure to tPTI-Bpin, but only without the *tert*-butyl moiety (Fig. 1a). Excitingly, through simple slow evaporation in different solutions, two crystalline polymorphs (tPTI-B1 and tPTI-B2) of tPTI-Bpin were cultured with different space groups of $P2_1/c$ and $P\bar{1}$, and one crystalline (PTI-B) of PTI-Bpin was obtained with the space group of $C2/c$. The tPTI-B1 crystal displayed the ML emission, while others are ML inactive. Interestingly, PTI-B had a similar molecular packing like tPTI-B2, and well explained their ML inactivity, further confirming the importance of molecular packing. Herein, we present the syntheses, ML characterizations,

^a Sauvage Center for Molecular Sciences, Department of Chemistry, Wuhan University, Wuhan 430072, China. E-mail: lizhen@whu.edu.cn, lichemlab@163.com; Fax: +86-27-68755767

^b Institute of Molecular Aggregation Science, Tianjin University, Tianjin 300072, China

† Electronic supplementary information (ESI) available: Synthetic procedures, NMR spectral data, photophysical properties, and single crystal X-ray analysis data. CCDC 1948484, 1948485 and 1948492. For ESI and crystallographic data in CIF or other electronic format see DOI: 10.1039/c9tc05218f

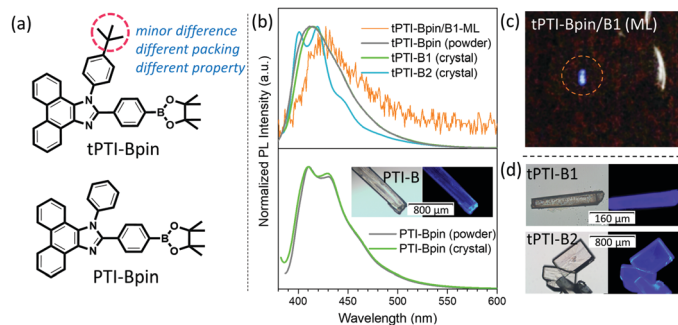


Fig. 1 (a) Chemical structures of tPTI-Bpin and PTI-Bpin. (b) ML spectrum of tPTI-Bpin, and PL spectra of tPTI-Bpin and PTI-Bpin in different states (inset: the images of crystal PTI-B by optical microscope Leica M123). (c) ML photo of tPTI-Bpin/B1. (d) The images of crystals tPTI-B1 and tPTI-B2 by optical microscope Leica M123, respectively.

crystal analyses and theoretical calculations of tPTI-Bpin and PTI-Bpin in detail, to understand the structure-packing-property relationship.

The synthetic routes of tPTI-Bpin and PTI-Bpin are illustrated in Scheme S1 (ESI[†]). The key intermediate compounds of tPTI-Br and PTI-Br were synthesized according to the literature.⁹ The target compounds were synthesized through the typical Miyaura Borylation reaction,¹⁰ and purified by silica gel chromatography followed by recrystallization. All the target compounds were characterized by ¹H and ¹³C NMR, mass spectrometry and elemental analysis. The thermogravimetric analysis (TGA) indicated the good thermal stability for tPTI-Bpin and PTI-Bpin, of which the decomposition temperatures (T_d) are 322 °C and 302 °C respectively (Fig. S2, ESI[†]). The UV-visible spectra of tPTI-Bpin and PTI-Bpin were measured in dilute tetrahydrofuran (THF) solution. As shown in Fig. S1 (ESI[†]), they have similar absorption spectra with two absorption bands centred at about 261 and 330 nm, which are attributed to the π - π^* local electron transition of the conjugated system. Similar photoluminescence (PL) spectra of tPTI-Bpin and PTI-Bpin in solution are also observed in Fig. S1 (ESI[†]) with the maximum emission wavelength at 397 and 386 nm, respectively.

The single crystals of tPTI-Bpin and PTI-Bpin were cultured by solvent evaporation at room temperature, with their structural data summarized in Table 1. Two polymorphs of tPTI-Bpin were obtained by changing the solvent mixture: prism-like crystal tPTI-B1 was grown from a solvent mixture of methanol and dichloromethane (DCM), another block-like crystal tPTI-B2 was from a solvent mixture of *n*-hexane and DCM. However, there was only stick-like crystal PTI-B obtained from different solvent mixtures for PTI-Bpin, which only lacks a *tert*-butyl

group on the outer phenyl ring compared to tPTI-Bpin. The morphology images of these crystals are shown in Fig. 1, which could be easily distinguished by the naked eye. All the three crystals emitted intense deep blue fluorescence under UV illumination at room temperature (Fig. 1b and Table 1). Crystal tPTI-B1 showed a similar emission spectrum to the powder of tPTI-Bpin, with the emission peaks locating at 414 and 411 nm, respectively. Crystal tPTI-B2 shows a different emission band shape with the main peak at 419 nm and a shoulder at 401 nm, due to its different molecular packing mode from that of tPTI-B1.^{3,11} Similar emission spectra were observed for crystal PTI-B and the powder of PTI-Bpin with the main emission peaks at 410 and 411 nm, respectively and the shoulders at 430 nm. Moreover, their PL quantum yields (ϕ_F) and fluorescence lifetimes (τ) were measured in solid states (Table 1 and Fig. S1, ESI[†]). The PL quantum yields of tPTI-Bpin in different solid states are generally higher than that of PTI-Bpin, and all of them have very short lifetimes ranging from 1.37 to 2.71 ns. When scraping the tPTI-B1 crystal or the crystalline powder of tPTI-Bpin at room temperature, bright blue emission centred at 427 nm could be observed without UV irradiation (Fig. 1b and c). However, no emission was observed for the tPTI-B2 or PTI-B crystal. This extremely opposite ML performance in different polymorphs of tPTI-Bpin should be related to the different molecular packing modes in the crystals, which should also account for the different ML properties of PTI-Bpin and tPTI-Bpin. To further explore the structure-ML property relationship, more investigations and analyses should be conducted based on single crystals and other experimental results.

The powder X-ray diffraction (PXRD) of the samples in different states was carried out. As readily seen, the as-prepared crystalline

Table 1 Optical properties and single crystal information of tPTI-Bpin and PTI-Bpin

	Emission (nm)	PLQY (%)	Lifetime (ns)	Crystal system	Space group	Symmetry	ML activity
tPTI-Bpin ^a	411	29.14	1.84	—	—	—	Inactive
tPTI-B1 ^b	414	36.62	1.38	Monoclinic	$P2_1/c$	Centrosymmetric	Active
tPTI-B2 ^b	419	58.04	2.71	Triclinic	$P\bar{1}$	Centrosymmetric	Inactive
PTI-Bpin ^a	411	14.94	1.84	—	—	—	Inactive
PTI-B ^b	410	10.72	1.37	monoclinic	$C2/c$	Centrosymmetric	Inactive

^a tPTI-Bpin and PTI-Bpin as prepared powder; ^b tPTI-Bpin and PTI-Bpin in the crystalline state.

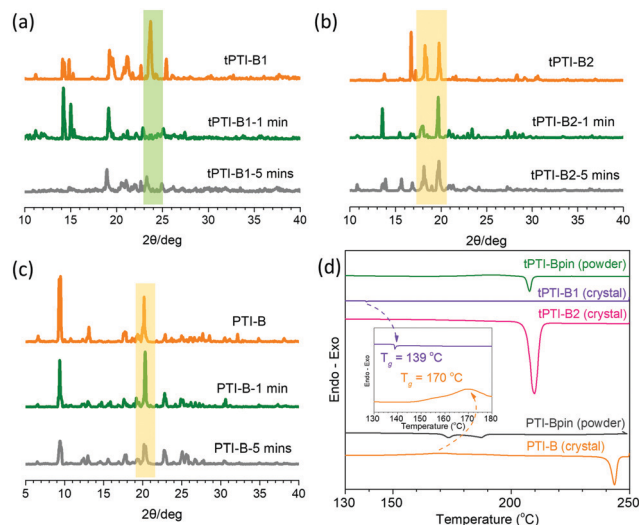


Fig. 2 The PXRD patterns of (a) tPTI-B1, (b) tPTI-B2, and (c) PTI-B in crystalline form, after grinding for 1 min and 5 min. (d) The DSC curves of tPTI-Bpin and PTI-Bpin in different states.

powders of tPTI-B1, tPTI-B2 and PTI-B all exhibited non-negligible peaks due to their good crystallinity (Fig. 2). Then, the as-prepared crystalline powders were ground for different durations by using a mortar and pestle to give two different degrees of grinding powders. For tPTI-B1, some diffraction peaks at around 24° disappeared after grinding for 1 minute. When 5 minutes of continuous grinding was conducted, almost all of the diffraction peaks disappeared. Accordingly, we could speculate that the lattice of the tPTI-B1 crystal is easily destroyed under mechanical stimulus, and the crystal is breakable to some extent. On the contrary, the sharp and high diffraction peaks of tPTI-B2 and PTI-B still remained even after grinding for 5 minutes, indicating their relatively high lattice stability and high hardness. The PXRD results could well demonstrate the different hardness and lattice stabilities of these crystals, which may affect their ML performances, since the ML process is often accompanied by crystal breakage. As depicted in the differential scanning calorimetry (DSC) curves, no obvious T_g was found for the tPTI-B2 crystal. The tPTI-B1 crystal showed a lower glass transition temperature (T_g) of 139°C than PTI-B (170°C), also indicating the higher lattice stability of PTI-B than that of tPTI-B1. The two polymorphs of tPTI-Bpin exhibited extremely opposite ML properties along with their different crystal lattice stabilities: the ML-active tPTI-B1 showed a relatively low lattice stability, while tPTI-B2 had a high lattice stability without the ML property. For another isomer of PTI-Bpin, its crystal PTI-B showed a similar high lattice stability and ML inactivity just like tPTI-B2. Thus, the ML properties were affected by the lattice stability of the crystals, which is highly related to the molecular packing and intermolecular interactions in the crystal.

The single crystal X-ray diffractions were carried out for PTI-B1, PTI-B2 and PTI-B, and the single crystal structure and molecular packing mode were carefully analyzed to investigate the deeper relationship between the crystal packing modes and ML performances. Table 1 and Table S5 (ESI[†]) show the basic

single crystal information of PTI-Bpin (PTI-B) and two polymorphs of tPTI-Bpin (tPTI-B1 and tPTI-B2). The space group of PTI-B is $C2/c$, while $P2_1/c$ for tPTI-B1 and $P\bar{1}$ for tPTI-B2, respectively. All of them are centrosymmetric, indicating that there are no piezoelectric effects in these crystals.^{4c,12} The intermolecular and intramolecular interactions in the unit cells of all three crystals were analysed carefully, with the results listed in Tables S1–S4 (ESI[†]). The single molecules in the three crystals all possess twisted structures, and the outer phenyl rings both twist towards the planar phenanthroimidazole (PTI) core with different torsion angles (Fig. S4, ESI[†]). Among them, tPTI-B1 possesses the most twisted structure with two torsion angles of 108.007° and 29.097° , respectively. Due to the different intramolecular interactions of the three crystals, the side *tert*-butylbenzene group in tPTI-B1 is closer to the PTI core, while the side phenyl rings in tPTI-B2 and PTI-B are closer to the aryl boronic ester moiety. Thus, tPTI-B1 demonstrated a totally different twisted conformation of a single molecule compared to tPTI-B2 and PTI-B, leading to different molecular packing modes of tPTI-B1 and tPTI-B2, and PTI-B (Fig. S3, ESI[†]).

As illustrated in Fig. 3a, there are three types of molecular dimers with efficient $\text{C-H}\cdots\text{O}$, $\text{C-H}\cdots\text{N}$ and $\text{C-H}\cdots\pi$ interactions existing in the unit cell of the ML active crystal tPTI-B1. Dimer-1 possesses an antiparallel conformation with 4 $\text{C-H}\cdots\pi$ ($3.593\text{--}3.633\text{ \AA}$) and 8 $\text{C-H}\cdots\text{O}$ ($2.663\text{--}3.987\text{ \AA}$) interactions. Dimer-2 displays a parallel conformation with 7 $\text{C-H}\cdots\pi$ ($2.693\text{--}3.971\text{ \AA}$) and 7 $\text{C-H}\cdots\text{N}$ ($2.746\text{--}3.975\text{ \AA}$) interactions. And molecules in dimer-3 stack in a nonparallel conformation with a certain angle and 11 $\text{C-H}\cdots\pi$ ($3.136\text{--}3.932\text{ \AA}$) and 4 $\text{C-H}\cdots\text{N}$ ($3.201\text{--}3.900\text{ \AA}$) interactions. With efficient intermolecular interactions, the three types of dimers form a triangle-like conformation in the unit cell of tPTI-B1, which is stable to some extent and

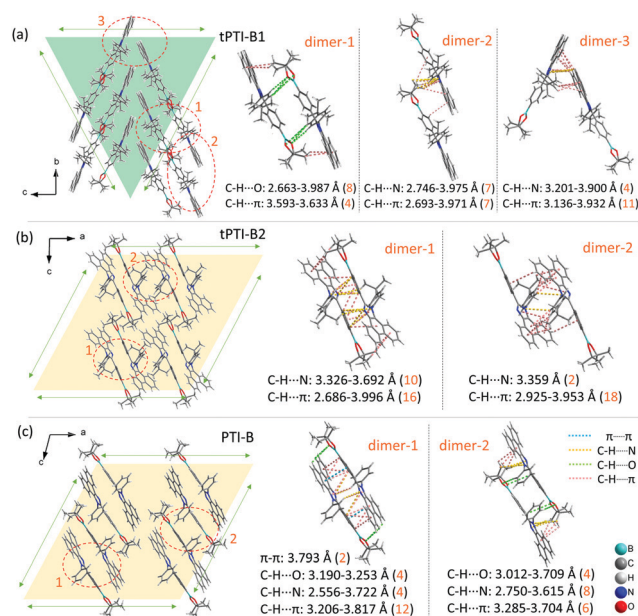


Fig. 3 The molecular packing and molecular dimers including intermolecular interactions in the unit cell of crystals (a) tPTI-B1, (b) tPTI-B2, and (c) PTI-B, respectively.

liable to breaking rather than slipping under a mechanical force. The ML inactive tPTI-B2 crystal, another polymorph of tPTI-Bpin, displays an extremely different molecular packing from tPTI-B1. In tPTI-B2, there are two types of molecular dimers in the unit cell, including dimer-1 with 16 C–H $\cdots\pi$ (2.686–3.996 Å) and 10 C–H $\cdots\text{N}$ (3.326–3.692 Å) interactions, and dimer-2 with 18 C–H $\cdots\pi$ (2.952–3.953 Å) and 2 C–H $\cdots\text{N}$ (3.359 Å) interactions. Dimer-1 and dimer-2 both possess similar antiparallel stacking to the dimer-1 in tPTI-B1, and also stack parallelly to each other, resulting in a parallelogram-like packing mode in the unit cell. When mechanical force is applied, tPTI-B2 with a parallelogram-like packing tends to generate a molecular slippage with the possible energy loss through a non-radiative relaxation route, resulting in its ML inactivity. However, since triangles are hard to slip rather than parallelograms, tPTI-B1 with the triangle-like packing is liable to breaking instead of slippage, effectively suppressing the non-radiative energy loss. Thus, the triangle-like packing mode of crystal tPTI-B1 should be partially responsible for its ML activity. A similar molecular packing mode to tPTI-B2 is found in the ML inactive PTI-B crystal, in which, the molecules also pack parallel to each other and form a parallelogram-like packing in the unit cell. And there are two molecular dimers including dimer-1 with 12 C–H $\cdots\pi$ (3.206–3.817 Å), 4 C–H $\cdots\text{N}$ (2.556–3.722 Å), 4 C–H $\cdots\text{O}$ (3.190–3.253 Å), and 2 $\pi\cdots\pi$ (3.793 Å) interactions, and dimer-2 with 6 C–H $\cdots\pi$ (3.285–3.704 Å), 8 C–H $\cdots\text{N}$ (2.750–3.615 Å), and 4 C–H $\cdots\text{O}$ (3.012–3.709 Å) interactions. Combined with the PXRD results, the different molecular packing modes and intermolecular interactions of these PTI derivatives could really affect the lattice stability and hardness of the crystals, resulting in different ML performances under mechanical stimulation.

As discussed above, in the two polymorphs of tPTI-Bpin (tPTI-B1 and tPTI-B2), the conformations of single molecules are very different, directly leading to their different molecular packing modes. As for the isomer of PTI-Bpin, it only lacks a *tert*-butyl group in the chemical structure compared to tPTI-Bpin, but the single crystal of PTI-Bpin displays a similar molecular packing mode as tPTI-B2. Thus, considering their chemical structures, molecular packing in the aggregated state, and emissive properties together, the molecular packing rather than the chemical structure mainly accounts for their different ML behaviors. The triangle-like molecular packing gives tPTI-B1 higher rigidity to realize the ML property, while the parallelogram-like molecular packing mode of tPTI-B2 and PTI-B is easy to slip under a mechanical force, leading to the increase of possible energy loss through non-radiative channels.

Density functional theory (DFT) calculations (B3LYP/6-31g(d,p)) were carried out on the isolated molecules (derived from their ground state geometries in single crystals). The molecules were in different conformations with different torsion angles between the peripheral phenyl rings and the central PTI core, which is well consistent with the molecular conformations in single crystal structures (Fig. 4). No distinct orbital delocalization was found on the isolated molecules, since there is no apparent D–A structure in these luminogens. Both the HOMO (the highest occupied molecular orbital) and

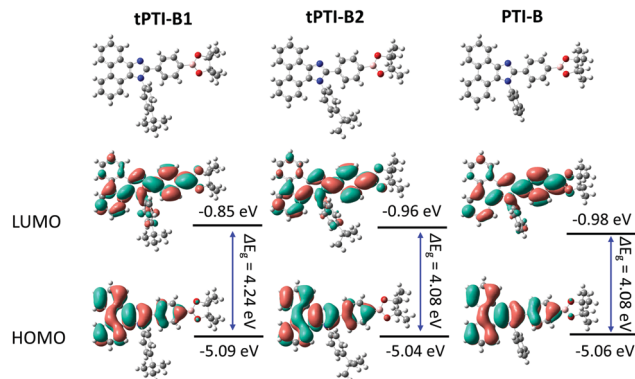


Fig. 4 The HOMO and LUMO of single molecules in tPTI-B1, tPTI-B2, and PTI-B calculated at the B3LYP/6-31G(d,p) level.

LUMO (the lowest unoccupied molecular orbital) delocalized on the PTI core and the phenyl ring linked to the carbon of PTI, indicating the weak intramolecular charge transfer in these luminogens.

In summary, two luminogens of tPTI-Bpin and PTI-Bpin with ignorable difference in the chemical structure have been designed and synthesized, to investigate the structure-packing-ML property relationship. The two crystalline polymorphs of tPTI-Bpin show opposite ML activities, derived from their different conformations of packing modes in the crystals. The crystal (PTI-B) of another isomer PTI-Bpin shows a similar molecular packing mode and ML inactivity to tPTI-B2, further confirming that the molecular packing rather than the chemical structure mainly accounts for their diverse ML properties. Therefore, the molecular packing is particularly important for the modulation of organic ML properties, which is of great significance for future research on organic ML materials.

Conflicts of interest

There are no conflicts to declare.

Acknowledgements

This work was supported by the National Natural Science Foundation of China (No. 51573140 and 21734007), Hubei Province (No. 2017CFA002) through financial support and the Special funds for basic scientific research services in central colleges and Universities (No. 2042017kf0247).

Notes and references

- (a) M. Berggren, A. Dodabalapur, R. E. Slusher and Z. Bao, *Nature*, 1997, **389**, 466; (b) B. Valeur, *Molecular Fluorescence: Principle and Applications*, Wiley, Weinheim, 2005; (c) R. B. Thompson, *Fluorescence Sensors and Biosensors*, CRC, Boca Raton, FL, 2006; (d) Y. Hong, J. W. Y. Lam and B. Z. Tang, *Chem. Commun.*, 2009, 4332; (e) D. Vaufrey, *OLED Microdisplays*, Wiley, Hoboken, 2014; (f) W. Wu, R. Tang, Q. Li and Z. Li, *Chem. Soc. Rev.*, 2015, **44**, 3997; (g) Z. Li, *Sci. China:*

- Chem.*, 2017, **60**, 1107; (h) Y. Song, L. Zong, L. Zhang and Z. Li, *Sci. China: Chem.*, 2017, **60**, 1596; (i) Z. Wang, J. Yang, Y. Yang, X. Xu, M. Li, Y. Zhang, H. Fang, H. Xu and S. Wang, *Chin. J. Org. Chem.*, 2018, **38**, 1401; (j) J. Yang, Z. Chi, W. Zhu, B. Z. Tang and Z. Li, *Sci. China: Chem.*, 2019, **62**, 1090; (k) L. Feng, C. Wang, X. Deng, X. Miao, J. Wang, Y. Wang and Z. Li, *Mater. Chem. Front.*, 2018, **2**, 264; (l) L. Zong, H. Zhang, Y. Li, Y. Gong, D. Li, J. Wang, Z. Wang, Y. Xie, M. Han, Q. Peng, X. Li, J. Dong, J. Qian, Q. Li and Z. Li, *ACS Nano*, 2018, **12**, 9532.
- 2 (a) B. Fraboni, A. Fraleoni-Margera, Y. Geerts, A. Morpurgo and V. Podzorov, *Adv. Funct. Mater.*, 2016, **26**, 2229; (b) A. Mannix, X. Zhou, B. Kiraly, J. Wood, D. Alducin, B. Myers, X. Liu, B. Fisher, U. Santiago, J. Guest, M. Yacaman, A. Ponce, A. Oganov, M. Hersam and N. Guisinger, *Science*, 2015, **350**, 1513; (c) Q. Li, Y. Tang, W. Hu and Z. Li, *Small*, 2018, **14**, 1801560; (d) X. Shao, *Sci. China: Chem.*, 2018, **61**, 975; (e) Z. Yang, Z. Chi, Z. Mao, Y. Zhang, S. Liu, J. Zhao, M. P. Aldred and Z. Chi, *Mater. Chem. Front.*, 2018, **2**, 861; (f) H. Liu, Y. Fu, W. Xu, Q. He, H. Cao, G. Liu and J. Cheng, *Sci. China: Chem.*, 2018, **61**, 857; (g) Q. Li and Z. Li, *Adv. Sci.*, 2017, **4**, 1600484; (h) C. Wang and Z. Li, *Mater. Chem. Front.*, 2017, **1**, 2174; (i) M. Fang, J. Yang, X. Xiang, Y. Xie, Y. Dong, Q. Peng, Q. Li and Z. Li, *Mater. Chem. Front.*, 2018, **2**, 2124; (j) M. Fang, J. Yang and Z. Li, *Chin. J. Polym. Sci.*, 2019, **37**, 383.
- 3 (a) X. Meng, B. Gui, D. Yuan, M. Zeller and C. Wang, *Sci. Adv.*, 2016, **2**, 1600480; (b) M. Baroncini, S. Agostino, G. Bergamini, P. Ceroni, A. Comotti, P. Sozzani, I. Bassanetti, F. Grepioni, T. Hernandez, S. Silvi, M. Venturi and A. Credi, *Nat. Chem.*, 2015, **7**, 634; (c) S. Mondal and G. Mugesh, *Angew. Chem.*, 2015, **127**, 10983; (d) M. Jin, T. Seki and H. Ito, *J. Am. Chem. Soc.*, 2017, **139**, 7452.
- 4 (a) J. I. Zink, *Acc. Chem. Res.*, 1978, **11**, 289; (b) A. J. Walton, *Adv. Phys.*, 1977, **26**, 887; (c) G. E. Hardy, W. C. Kaska, B. P. Chandra and J. I. Zink, *J. Am. Chem. Soc.*, 1981, **103**, 1074; (d) S. M. Jeong, S. Kim, H. Kim, K. I. Joo and H. Takezoe, *Adv. Funct. Mater.*, 2016, **26**, 4848; (e) M. P. Brenner, S. Hilgenfeldt and D. Lohse, *Rev. Mod. Phys.*, 2002, **74**, 425.
- 5 (a) Y. Xie and Z. Li, *Chem*, 2018, **4**, 943; (b) D. Tu, C. N. Xu, A. Yoshida, M. Fujihala, J. Hirotsu and X. G. Zheng, *Adv. Mater.*, 2017, **29**, 1606914; (c) E. Ubba, Y. Tao, Z. Yang, J. Zhao, L. Wang and Z. Chi, *Chem. – Asian J.*, 2018, **13**, 3106; (d) Y. Xie, J. Tu, T. Zhang, J. Wang, Z. Xie, Z. Chi, Q. Peng and Z. Li, *Chem. Commun.*, 2017, **53**, 11330; (e) J. Mei, N. L. C. Leung, R. T. K. Kwok, J. W. Y. Lam and B. Z. Tang, *Chem. Rev.*, 2015, **115**, 11718; (f) M. L. Liu, Q. Wu, H. F. Shi, Z. F. An and W. Huang, *Acta Chim. Sin.*, 2018, **76**, 246; (g) J. I. Zink and W. Klimt, *J. Am. Chem. Soc.*, 1974, **96**, 4690; (h) R. Nowak, A. Krajewska and M. Samoc, *Chem. Phys. Lett.*, 1983, **94**, 270; (i) L. M. Sweeting, A. L. Rheingold, J. M. Gingerich, A. W. Rutter, R. A. Spence, C. D. Cox and T. J. Kim, *Chem. Mater.*, 1997, **9**, 1103; (j) X. Gao, *Sci. China: Chem.*, 2018, **61**, 641; (k) M. Fang, J. Yang, Q. Liao, Y. Gong, Z. Xie, Z. Chi, Q. Peng, Q. Li and Z. Li, *J. Mater. Chem. C*, 2017, **5**, 9879; (l) J. Tu, F. Liu, J. Wang, X. Li, Y. Gong, Y. Fan, M. Han, Q. Li and Z. Li, *ChemPhotoChem*, 2019, **3**, 133.
- 6 (a) C. Wang, B. Xu, M. Li, Z. Chi, Y. Xie, Q. Li and Z. Li, *Mater. Horiz.*, 2016, **3**, 220; (b) B. Xu, J. He, Y. Mu, Q. Zhu, S. Wu, Y. Wang, Y. Zhang, C. Jin, C. Lo, Z. Chi, A. Lien, S. Liu and J. Xu, *Chem. Sci.*, 2015, **6**, 3236; (c) Z. Xie, T. Yu, J. Chen, E. Ubba, L. Wang, Z. Mao, T. Su, Y. Zhang, M. P. Aldred and Z. Chi, *Chem. Sci.*, 2018, **9**, 5787; (d) C. Wang, Y. Yu, Z. Chai, F. He, C. Wu, Y. Gong, M. Han, Q. Li and Z. Li, *Mater. Chem. Front.*, 2019, **3**, 32.
- 7 (a) F. Liu, J. Tu, X. Wang, Y. Gong, M. Han, X. Dang, Q. Liao, Q. Peng, Q. Li and Z. Li, *Chem. Commun.*, 2018, **54**, 5598; (b) Y. Xie and Z. Li, *Chem. – Asian J.*, 2019, **14**, 2524.
- 8 (a) J. Yang, Z. Ren, Z. Xie, Y. Liu, C. Wang, Y. Xie, Q. Peng, B. Xu, W. Tian, F. Zhang, Z. Chi, Q. Li and Z. Li, *Angew. Chem., Int. Ed.*, 2017, **56**, 880; (b) Y. Gong, P. Zhang, Y. Gu, J. Wang, M. Han, C. Chen, X. Zhan, Z. Xie, B. Zhou, Q. Peng, Z. Chi and Z. Li, *Adv. Opt. Mater.*, 2018, **61**, 641; (c) T. Wang, N. Zhang, K. Zhang, J. Dai, W. Bai and R. Bai, *Chem. Commun.*, 2016, **52**, 9679; (d) Q. Sun, L. Tang, Z. Zhang, K. Zhang, Z. Xie, Z. Chi, H. Zhang and W. Yang, *Chem. Commun.*, 2018, **54**, 94; (e) Q. Dang, L. Hu, J. Wang, Q. Zhang, M. Han, S. Luo, Y. Gong, C. Wang, Q. Li and Z. Li, *Chem. – Eur. J.*, 2019, **25**, 7031.
- 9 (a) Z. Wang, P. Lu, S. Chen, Z. Gao, F. Shen, W. Zhang, Y. Xu, H. S. Kwok and Y. Ma, *J. Mater. Chem.*, 2011, **21**, 5451; (b) W. Li, D. Liu, F. Shen, D. Ma, Z. Wang, T. Feng, Y. Xu, B. Yang and Y. Ma, *Adv. Funct. Mater.*, 2012, **22**, 2797; (c) P. Gu, Z. Wang and Q. Zhang, *J. Mater. Chem. B*, 2016, **4**, 7060; (d) J. Li, P. Li, J. Wu, J. Gao, W. Xiong, G. Zhang, Y. Zhao and Q. Zhang, *J. Org. Chem.*, 2014, **79**, 4438.
- 10 T. Ishiyama, M. Murata and N. Miyaura, *J. Org. Chem.*, 1995, **60**, 7508.
- 11 (a) C. Zheng, Q. Zang, H. Nie, W. Huang, Z. Zhao, R. Hu and B. Z. Tang, *Mater. Chem. Front.*, 2018, **2**, 180; (b) H. Liu, Q. Bai, L. Yao, H. Zhang, H. Xu, S. Zhang, W. Li, Y. Gao, J. Li, P. Liu, H. Wang, B. Yang and Y. Ma, *Chem. Sci.*, 2015, **6**, 3797; (c) B. Yang, J. Xiao, J. I. Wong, J. Guo, Y. Wu, L. Ong, L. L. Lao, F. Boey, H. Zhang, H. Y. Yang and Q. Zhang, *J. Phys. Chem. C*, 2011, **115**, 7924; (d) Y. Li, W. Wang, Z. Zhuang, Z. Wang, G. Lin, P. Shen, S. Chen, Z. Zhao and B. Z. Tang, *J. Mater. Chem. C*, 2018, **6**, 5900; (e) Z. Gao, C. Wei, Y. Han, M. Yuan, X. Yan and F. Wang, *Chin. J. Polym. Sci.*, 2018, **36**, 399; (f) L. Hu, L. Li, Y. Yang, T. Guo, Y. Zhang, W. Yang and Y. Cao, *Chin. J. Polym. Sci.*, 2018, **36**, 546; (g) Y. Xie, Y. Ge, Q. Peng, C. Li, Q. Li and Z. Li, *Adv. Mater.*, 2017, **29**, 1606829; (h) J. Yang, X. Zhen, B. Wang, X. Gao, Z. Ren, J. Wang, Y. Xie, J. Li, Q. Peng, K. Pu and Z. Li, *Nat. Commun.*, 2018, **9**, 840; (i) Q. Li and Z. Li, *Sci. China Mater.*, 2019, DOI: 10.1007/s40843-019-1172-2.
- 12 (a) B. P. Chandra, M. Elyas, K. K. Shrivastava and R. D. Verma, *Solid State Commun.*, 1980, **36**, 931; (b) B. P. Chandra, V. K. Chandra and P. Jha, *J. Lumin.*, 2013, **135**, 139.